

COMPARATIVE STUDY OF FLUORIDE CONVERSION COATING STRUCTURE ON TWO TYPES OF BULK MAGNESIUM MATERIALS

¹Roman BRESCHER, ¹Matěj BŘEZINA, ²Juliána DZIKOVÁ, ¹Jaromír WASSERBAUER, ¹Jan STANĚK

¹*Institute of materials science, Faculty of Chemistry, Brno University of Technology, Brno, Czech Republic, EU, roman.brescher@vut.cz, brezina@fch.vut.cz, wasserbauer@fch.vut.cz, jan.stanek4@vut.cz*

²*Research Centre of the University of Žilina, University of Žilina, Žilina, Slovak Republic, EU, juliana.dzikova@uniza.sk*

<https://doi.org/10.37904/metal.2021.4201>

Abstract

This paper deals with the structural and composition differences of two types of fluoride conversion coatings on two types of bulk magnesium materials. The bulk magnesium materials used were powder metallurgy cold compacted magnesium and sintered magnesium materials. One type of coating was prepared by dipping the magnesium samples in hydrofluoric acid and the second one by immersing the samples in Na[BF₄] molten salt. Microstructure and elemental composition were examined by scanning electron microscope equipped with an EDS analyzer. The phase composition was analyzed using an XRD. The fluoride conversion coating prepared from Na[BF₄] molten salt grew significantly deeper into the cold compacted magnesium than to the sintered material. Also, traces of fluorine were found inside the bulk of cold compacted material, while no fluorine traces were found inside the sintered material. The coating prepared from hydrofluoric acid appeared the same in both magnesium materials, with similar depth and fluorine traces found inside the bulk of both of the materials. Furthermore, the coating prepared from Na[BF₄] molten salt grew deeper into the material than the coating prepared from hydrofluoric acid. The differences between the two coatings in creation depth, structures, and layout of fluorine inside the material suggest a difference in the creation mechanism of the two coatings.

Keywords: Powder metallurgy, fluoride conversion coating, magnesium, EDS mapping

1. INTRODUCTION

Magnesium alloys have great potential for medical applications, such as manufacturing temporary bone implants, stents and sutures. This is mainly due to their low density and suitable mechanical properties [1]. Furthermore, mechanical and chemical properties can be further improved via various powder metallurgy techniques. However, what distinguishes magnesium alloys from other metal alloys for biomedical applications is their biodegradability. Magnesium implants can theoretically gradually dissolve in the body after fulfilling their purpose. Although slow decomposition of the implant is desirable, most magnesium alloys decompose too fast in the physiological environment [2]. This may lead to the loss of mechanical properties of the implant before accomplishing its intended function. Less apparent consequences of rapid magnesium degradation are a local increase of magnesium ions and the evolution of hydrogen, which may lead to the separation of the tissue from the implant [3]. Slowing down the corrosion of magnesium implants is the key issue to be solved. One of the possible solutions is a surface coating that may increase the corrosion resistance of the material. However, not every coating is acceptable in medical applications [4].

One option is the creation of a fluoride conversion coating. Previous studies have shown that this type of coating might slow down the corrosion rate of magnesium alloys in the environment of simulated body fluids [5]. It was also proven that such an increase in corrosion resistance lowers the rate of hydrogen production

and lowers magnesium ions concentration in the vicinity of the implant [6]. In addition to that, fluoride anions can support osteoblast growth help the bone heal [7][7]. Fluoride conversion coating also allows the application of more bioactive coatings by improving their adhesion to the substrate [8]. There are two possible ways to produce fluoride conversion coating on magnesium alloys. The more conventional one is by dipping the magnesium-based material into the HF solution. Coating prepared in this manner contains MgF_2 and a relatively small amount of MgO [9]. The other, rather unconventional way of preparing fluoride conversion coating is immersing the material in the $Na[BF_4]$ molten salt. The outcome of this preparation is a coating made of MgF_2 and a secondary layer of $Na[MgF_3]$ [10]. Previous studies have shown that the less conventional way of preparing the coating has superior corrosion properties on AZ61 magnesium alloy [11]. The fluoride coatings were tested on magnesium alloys but not on materials prepared via powder metallurgy. This study focuses on preparing both types of fluoride coatings on cold compacted magnesium and sintered magnesium.

2. EXPERIMENTAL

Magnesium prepared by two different ways of powder metallurgy (cold compacted and sintered) served as the substrate. Magnesium powder was supplied by (goodfellow) and had a declared purity of 99,8 %. The average powder particle size was 27,6 μm . Base material was weighted and poured into cylindrical steel dies with an inner diameter of 20 mm in a nitrogen atmosphere. The dies were sealed and then axially pressed at a rate of $1 \text{ mm} \cdot \text{min}^{-1}$ until a pressure reached 400 MPa with a holding time of 60 s at maximum pressure. The height of the resulting magnesium cylinder was approximately 5 mm. The samples for sintering were sintered in an argon atmosphere at a temperature of 620 °C for 20 h and then let cool in the furnace.

Coating of samples in HF was prepared by dipping them in concentrated HF for 24 hours at laboratory temperature. Samples coated in this manner were rinsed in distilled water, isopropanol and dried in the stream of hot air. Preparation of coatings by immersion in molten $Na[BF_4]$ begun with melting the salt itself in a furnace inside a corundum crucible at 450 °C. After the melt had tempered, samples were submerged into it for 4 h and kept at 450 °C. The samples were taken out of the melt and cool freely in the air after the coating process was finished. To get rid of the residual salt and $Na[MgF_3]$ secondary layer, the samples were boiled in distilled water for 1 h after they cooled down.

A Zeiss Evo LS-10 with an OXFORD X-Max 80 mm^2 energy dispersive spectroscopy (EDS) analyzer was used to analyze the elemental composition of the cross-section of the metallographic cut of the samples. The accelerating voltage during the measurement was 15 kV. Qualitative analysis of the phase composition of the prepared coatings was performed by x-ray diffraction (XRD) analysis on an instrument from SmartLab. The measurement took place in the range of $5^\circ - 90^\circ$ with a step size of 0.02° . The diffractograms were evaluated using the JCPDS PDF-4 database.

3. RESULTS AND DISCUSSION

Figure 1 and **Figure 2** shows EDS maps of the cross-section of cold compacted specimens coated by fluoride conversion coating prepared by immersion in molten $Na[BF_4]$ and by dipping in HF, respectively. It is apparent that coating went relatively deep into the material. In the case of preparation via $Na[BF_4]$ shown in (**Figure 1**), the coating is coherent and goes approximately 150 μm into the material. On the other hand, coating prepared via HF, which is shown in (**Figure 2**) is much thinner on the surface (up to approximately 10 μm), but traces of fluorine can be found deep within the material. According to a previous study on the mechanism of formation of fluoride conversion coating, BF_3 forms by thermal decomposition of $Na[BF_4]$ and serves as the source of fluorine [10]. In the case of preparation via HF, the source of fluorine is much smaller fluoride anions. This might mean that diffusion is much easier in the case of fluoride anions and goes deeper into the material. The EDS maps of oxygen layout in the material indicate that magnesium oxides are present throughout the material. This was expected, as magnesium readily oxidizes even at room temperatures and oxides might have formed during the specimen preparation [12]. Low concentration of oxygen in (**Figure 1c**) indicates that

the fluorine from the salt decomposition reacted with the present magnesium oxides to form magnesium fluoride as the apparent concentration of oxygen at the surface of the specimen is lower than in the concentration deeper in the cross-section of the material. **Figure 1d** shows the presence of the sodium layer. This may indicate the presence of the secondary layer of $\text{Na}[\text{MgF}_3]$ on the top of the coated sample. The presence of sodium only on the sample's surface also indicates that the salt melt did not penetrate into the material. This supports the theory that the coating is not created by the direct reaction of magnesium with the salt itself but rather with the products of decomposition of the salt [10]. However, the proposed reaction in the literature counts BF_3 molecule as one of the reactants responsible for the coating preparation, which in this case is probably not possible because no traces of boron were found in the material. The initial coating formation on the surface of the sample may form according to the proposed equation, but the amount of fluorine in the material and lack of boron and sodium indicates that the MgF_2 formed in the depth of the material is formed by the reaction of fluorine anion rather than the BF_3 molecule.

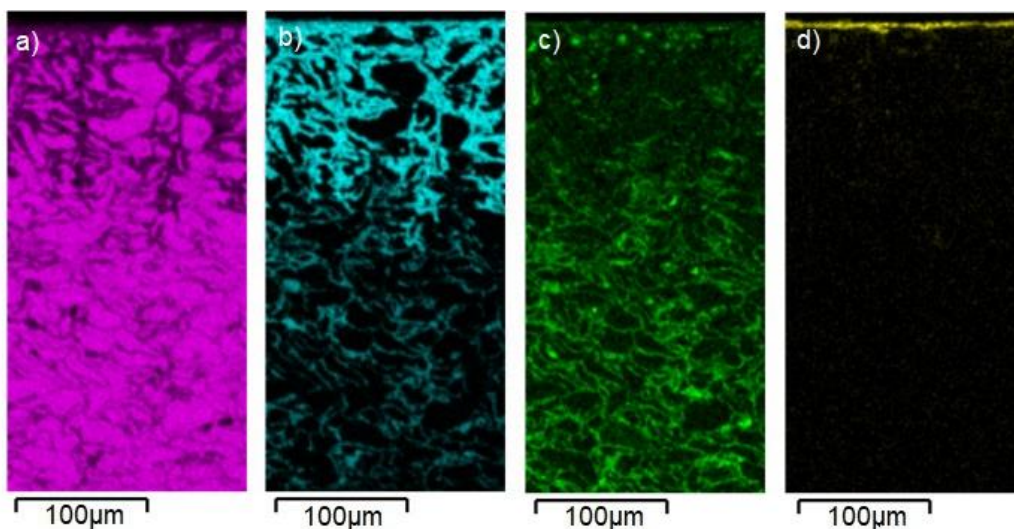


Figure 1 EDS maps of the cross-section of cold compacted magnesium coated by immersion in molten $\text{Na}[\text{BF}_4]$ where a) is Mg, b) is F, c) is O and d) is Na

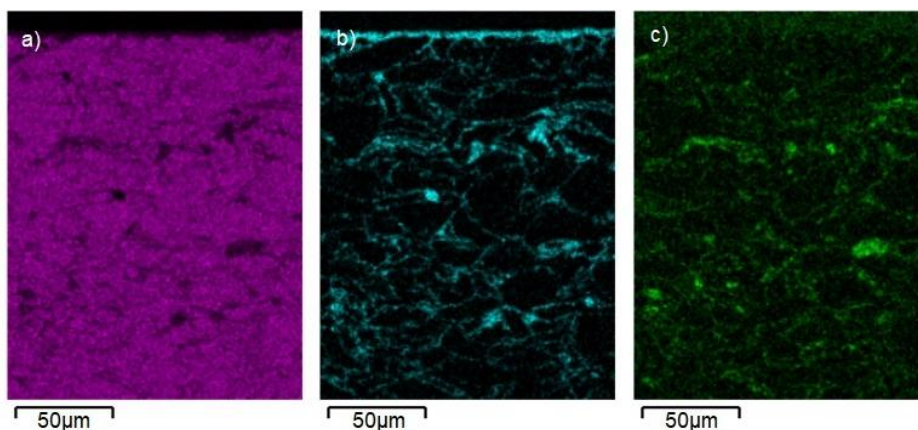


Figure 2 EDS maps of the cross-section of cold compacted magnesium coated by dipping in HF where a) is Mg, b) is F and c) is O

Figure 3 and **Figure 4** show EDS maps of the cross-section of sintered specimens coated by fluoride conversion coating prepared by immersion in molten $\text{Na}[\text{BF}_4]$ and by dipping in HF, respectively. Coating prepared in HF shown in (**Figure 4**) has similar characteristics regarding its depth and composition as the

coating shown in **(Figure 2)**. Traces of fluorine were found inside the bulk of the material in both cases and in a similar amount. Therefore, we can conclude that the state of the base material does not have an apparent effect on the quality of the coating prepared by dipping in HF. However, there are apparent differences in the depth of coating prepared by immersion in molten Na[BF₄] salt on cold compacted and sintered material. According to the EDS map in **(Figure 3b)**, the coating goes to the depth of approximately 50 μm. Furthermore, in contrast with this type of coating prepared on cold compacted material, no traces of fluorine were found inside the material itself. This was probably due to pore closure due to sintering, where the fluorine source from the Na[BF₄] molten salt could not diffuse into the material. The sodium layer is visible in **(Figure 3d)**. Although this layer is the same on both types of material, it has nothing to do with the state of the base material, but only with the post-processing of the conversion coating.

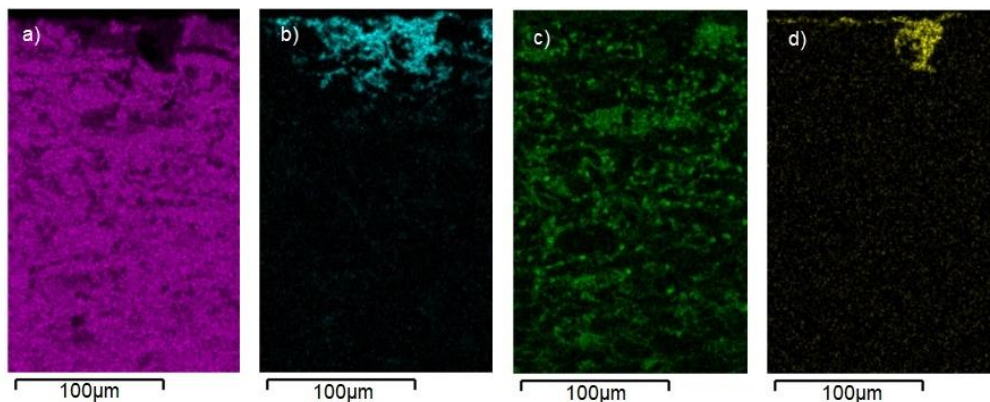


Figure 3 EDS maps of the cross-section of sintered magnesium coated by immersion in molten Na[BF₄] where a) is Mg, b) is F, c) is O and d) is Na

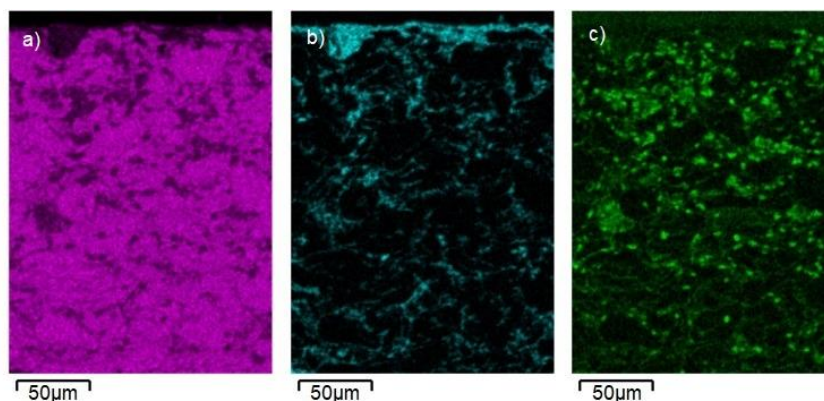


Figure 4 EDS maps of the cross-section of sintered magnesium coated by dipping in HF where a) is Mg, b) is F and c) is O

Qualitative measurements of coated sintered magnesium samples were performed by an XRD. The XRD spectra are shown in **(Figure 5)**. Peaks indicating the presence of magnesium, magnesium oxide, and magnesium nitride are present in all of the specimens, regardless of the way of coating preparation. Magnesium nitride was most probably formed during sintering, as magnesium undergoes nitridation at elevated temperatures in a nitrogen atmosphere [13]. Although sintering itself was performed in the argon atmosphere, residual nitrogen could be trapped between individual grains of magnesium during the pressing of specimens. The presence of oxygen has already been detected by EDS analysis and XRD analysis confirmed the presence of magnesium oxides.

The conversion coating of MgF_2 was detected on all of the specimens. However, XRD analysis shows some differences in crystal size between the two types of coatings. **Figure 5a** shows the XRD spectrum of magnesium coated by dipping in HF. Characteristic peaks of MgF_2 coating are short and wide in comparison to the peaks of MgF_2 shown for coating prepared via immersion in the molten $Na[BF_4]$ salt in (**Figure 5b**). This might mean that MgF_2 crystals formed via HF are much finer than crystals formed by the unconventional coating method. Previous studies have shown that size of crystals of some coatings has an influence on their corrosion protection, where bigger crystals have better corrosion characteristics [14]. Therefore, this may be a contributing factor to the improved corrosion resistance of the unconventionally prepared fluoride conversion coating shown in the previous study [11]. The XRD spectrum in (**Figure 5b**) also shows the presence of a secondary layer of $Na[MgF_3]$. This layer is under suspicion of its toxicity and although it was not proven yet, the secondary layer needs to be removed entirely for real-life application. It is apparent that boiling the specimen in water was not sufficient, and more time is required. XRD detected no residual $Na[BF_4]$ salt.

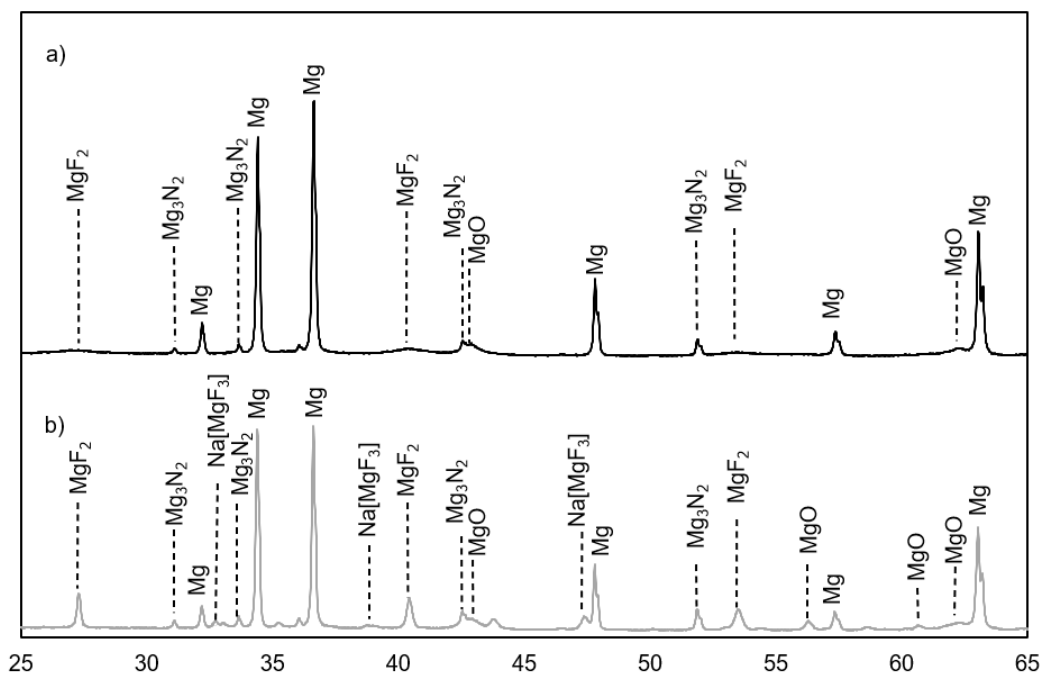


Figure 5 XRD spectra of sintered magnesium coated in a) HF and b) molten $Na[BF_4]$ salt

4. CONCLUSIONS

This paper compares fluoride conversion coatings prepared in two distinct ways on pure magnesium specimens prepared via powder metallurgy methods. The elemental and phase composition of both coatings were investigated. Based on the results, these conclusions can be drawn:

Both ways of coating preparation led to the MgF_2 fluoride coating formation. Notable differences were in crystallographic composition and the presence of a secondary layer in the case of the coating prepared from the salt melt.

In the case of the coating prepared from hydrofluoric acid, the state of the magnesium material had no apparent effect on the depth to which the coating was created.

In the case of the coating prepared from the salt melt, the state of the magnesium had a significant effect on the depth to which the coating was created.

Even though the chemical composition of the fluoride coating is the same, the differences in the layout of fluorine and crystallography show that the creation mechanism of the individual coatings is different.

ACKNOWLEDGEMENTS

This work was supported by Specific University Research at FCH BUT, Project Nr. FCH-S-21-7553, Ministry of Education, Youth and Sports of the Czech Republic.

REFERENCES

- [1] HARANDI, S.E.; SINGH RAMAN, R.K. Appropriate Mechanochemical Conditions for Corrosion-Fatigue Testing of Magnesium Alloys for Temporary Bioimplant Applications. *The Minerals, Metals & Materials Society*. [online]. 2015, vol. 67 pp. 1137-1142. Available from: <https://doi.org/10.1007/s11837-015-1387-7>.
- [2] WITTE, F.; FISCHER, J.; NELLESEN, J.; CROSTACK, H.-A.; KAESE, V.; PISCH, A.; BECKMANN, F.; WINDHAGEN, H. In vitro and in vivo corrosion measurements of magnesium alloys. *Biomaterials*. [online]. 2006, vol. 27, pp. 1013-1018. Available from: <https://doi.org/10.1016/j.biomaterials.2005.07.037>.
- [3] ZHEN, Z.; LIU, X.; HUANG, T.; XI, T.F.; ZHENG, Y. Hemolysis and cytotoxicity mechanisms of biodegradable magnesium and its alloys. *Materials Science and Engineering*. [online]. 2015, vol. 46, pp. 202-206. Available from: <https://doi.org/10.1016/j.msec.2014.08.038>.
- [4] HORNBERGER, H.; VIRTANEN, S.; BOCCACCINI, A.R. Biomedical coatings on magnesium alloys – A review. *Acta Biomaterialia*. [online]. 2012, vol. 8, pp. 2442-2455. Available from: <https://doi.org/10.1016/j.actbio.2012.04.012>.
- [5] YAN, T.; TAN, L.; XIONG, D.; LIU, X.; ZHANG, B.; YANG, K. Fluoride treatment and in vitro corrosion behavior of an AZ31B magnesium alloy. *Materials Science and Engineering*. [online]. 2010, vol. 30, pp. 740-748. Available from: <https://doi.org/10.1016/j.msec.2010.03.007>.
- [6] TIAN, P.; PENG, F.; WANG, D.; LIU, X. Corrosion behavior and cytocompatibility of fluoride-incorporated plasma electrolytic oxidation coating on biodegradable AZ31 alloy. *Regenerative Biomaterials*. [online]. 2017, vol. 4, pp. 1-10. Available from: <https://doi.org/10.1093/rb/rbw036>.
- [7] SUN, W.; ZHANG, G.; TAN, L.; YANG, K.; AI, H. The fluoride coated AZ31B magnesium alloy improves corrosion resistance and stimulates bone formation in rabbit model. *Materials Science and Engineering*. [online]. 2016, vol. 63. Available from: <https://doi.org/10.1016/j.msec.2016.03.016>.
- [8] SANKARA NARAYANAN, T.S.N.; PARK, I.S.; LEE, M.H. Tailoring the composition of fluoride conversion coatings to achieve better corrosion protection of magnesium for biomedical applications. *J. Mater. Chem.* [online]. 2014, vol. 2, pp. 3365-3382. Available from: <https://doi.org/10.1039/C3TB21565B>.
- [9] YAN, T.; TAN, L.; ZHANG, B.; YANG, K. Fluoride Conversion Coating on Biodegradable AZ31B Magnesium Alloy. *Journal of Materials Science & Technology*. [online]. 2014, vol. 30, pp. 666-674. Available from: <https://doi.org/10.1016/j.jmst.2013.12.015>.
- [10] DRÁBIKOVÁ, J.; FINTOVÁ, S.; PTÁČEK, P.; KUBĚNA, I.; BŘEZINA, M.; WASSERBAUER, J.; DOLEŽAL, P.; PASTOREK, F. Structure and growth kinetic of unconventional fluoride conversion coating prepared on wrought AZ61 magnesium alloy. *Surface and Coatings Technology*. [online]. 2020, vol. pp. 399. Available from: <https://doi.org/10.1016/j.surfcoat.2020.126101>.
- [11] DRÁBIKOVÁ, J.; FINTOVÁ, S.; TKACZ, J.; DOLEŽAL, P.; WASSERBAUER, J. Unconventional fluoride conversion coating preparation and characterization. *Anti-Corrosion Methods and Materials*. [online]. 2017, vol. 64, pp. 613-619. Available from: <https://doi.org/10.1108/ACMM-02-2017-1757>.
- [12] CZERWINSKI, F. Oxidation Characteristics of Magnesium Alloys. *JOM*. [online]. 2012, vol. 64, pp. 1477-1483. Available from: <https://doi.org/10.1007/s11837-012-0477-z>.
- [13] CHUNMIAO, Y.; LIFU, Y.; CHANG, L.; GANG, L.; SHENGJUN, Z. Thermal analysis of magnesium reactions with nitrogen/oxygen gas mixtures. *Journal of Hazardous Materials*. [online]. 2013, vol. 260, pp. 707-714. Available from: <https://doi.org/10.1016/j.jhazmat.2013.06.047>.
- [14] R. LÓPEZ, J. The Effect of Boron Content, Crystal Structure, Crystal Size on the Hardness and the Corrosion Resistance of Electrodeposited Ni-B Coatings. *International Journal of Electrochemical Science*. [online]. 2016, pp. 4231-4244. Available from: <https://doi.org/10.20964/2016.06.23>.